Biogeosciences, 10, 4847–4859, 2013
www.biogeosciences.net/10/4847/2013/
doi:10.5194/bg-10-4847-2013

Biogeosciences Open Access

Pelagic community production and carbon-nutrient stoichiometry under variable ocean acidification in an Arctic fjord

A. Silyakova[1,2], R. G. J. Bellerby[1,2,3,4], K. G. Schulz[5,6], J. Czerny[5], T. Tanaka[7,8], G. Nondal[1,2,3], U. Riebesell[5], A. Engel[5], T. De Lange[3,4], and A. Ludvig[5]

[1]Uni Bjerknes Centre, Allégaten 55, 5007 Bergen, Norway
[2]Bjerknes Center for Climate Research, Allégaten 55, 5007 Bergen, Norway
[3]Norwegian Institute for Water Research, Thormøhlensgate 53 D, 5006 Bergen, Norway
[4]Geophysical Institute, University of Bergen, Allégaten 70, 5007 Bergen, Norway
[5]Helmholtz Centre for Ocean Research Kiel (GEOMAR), Düsternbrooker Weg 20, 24105 Kiel, Germany
[6]Centre for Coastal Biogeochemistry, School of Environmental Science and Management, Southern Cross University, P.O. Box 157, Lismore, NSW 2480, Australia
[7]INSU-CNRS, Laboratoire d'Océanographie de Villefranche, BP 28, 06234 Villefranche sur Mer cedex, France
[8]Université Pierre et Marie Curie-Paris 6, Observatoire Océanologie de Villefranche, 06230 Villefranche sur Mer cedex, France

Correspondence to: R. G. J. Bellerby (richard.bellerby@niva.no)

Received: 30 July 2012 – Published in Biogeosciences Discuss.: 30 August 2012
Revised: 3 June 2013 – Accepted: 5 June 2013 – Published: 17 July 2013

Abstract. Net community production (NCP) and carbon to nutrient uptake ratios were studied during a large-scale mesocosm experiment on ocean acidification in Kongsfjorden, western Svalbard, during June–July 2010. Nutrient depleted fjord water with natural plankton assemblages, enclosed in nine mesocosms of $\sim 50\,m^3$ in volume, was exposed to pCO_2 levels ranging initially from 185 to 1420 µatm. NCP estimations are the cumulative change in dissolved inorganic carbon concentrations after accounting for gas exchange and total alkalinity variations. Stoichiometric coupling between inorganic carbon and nutrient net uptake is shown as a ratio of NCP to a cumulative change in inorganic nutrients. Phytoplankton growth was stimulated by nutrient addition half way through the experiment and three distinct peaks in chlorophyll *a* concentration were observed during the experiment. Accordingly, the experiment was divided in three phases. Cumulative NCP was similar in all mesocosms over the duration of the experiment. However, in phases I and II, NCP was higher and in phase III lower at elevated pCO_2. Due to relatively low inorganic nutrient concentration in phase I, C : N and C : P uptake ratios were calculated only for the period after nutrient addition (phase II and phase III). For the total post-nutrient period (phase II + phase III) ratios were close to Redfield, however they were lower in phase II and higher in phase III. Variability of NCP, C : N and C : P uptake ratios in different phases reflects the effect of increasing CO_2 on phytoplankton community composition and succession. The phytoplankton community was composed predominantly of haptophytes in phase I, prasinophytes, dinoflagellates, and cryptophytes in phase II, and haptophytes, prasinophytes, dinoflagellates and chlorophytes in phase III (Schulz et al., 2013). Increasing ambient inorganic carbon concentrations have also been shown to promote primary production and carbon assimilation. For this study, it is clear that the pelagic ecosystem response to increasing CO_2 is more complex than that represented in previous work, e.g. Bellerby et al. (2008). Carbon and nutrient uptake representation in models should, where possible, be more focused on individual plankton functional types as applying a single stoichiometry to a biogeochemical model with regard to the effect of increasing pCO_2 may not always be optimal. The phase variability in NCP and stoichiometry may be better understood if CO_2 sensitivities of the plankton's functional type biogeochemical uptake kinetics and trophic interactions are better constrained.

Published by Copernicus Publications on behalf of the European Geosciences Union.

1 Introduction

The Arctic Ocean is a key player in global carbon cycling (e.g. Bates et al., 2009) and the Arctic shelves are currently amongst the most productive areas of the world's oceans (Wassmann et al., 2011). Over the past decades, the Arctic Ocean has experienced significant change (e.g. Christensen et al., 2007 and references therein) including warming (Loeng, 2005, Trenberth et al., 2007), sea-ice decline (Polyakov et al., 2010; Stroeve et al., 2012), freshening (McPhee et al., 2009 and reference therein) and increasing surface carbon dioxide (CO_2) concentrations (Cai et al., 2010) with concomitant ocean acidification (Bellerby et al., 2005; Yamamoto-Kawai et al., 2009, 2011).

Due to naturally low carbonate ion concentrations and thus a lower buffer capacity than most of the global ocean, rapid ocean warming, diminishing ice cover facilitating greater ocean CO_2 uptake and a rapidly increasing freshwater fraction, waters of the Arctic Ocean are and will continue to exhibit the fastest rate of ocean acidification of all the world's oceans (Bellerby et al., 2005; Steinacher et al., 2009). Undersaturation with respect to aragonite is already found in surface waters of the Canada Basin (Yamamoto-Kawai et al., 2009; Chierici et al., 2009; Bates et al., 2012). Model studies show that the Arctic Ocean may become entirely undersaturated with respect to aragonite already by 2050 (Anderson et al., 2010).

These chemical changes may induce modifications in organism physiology and ecosystem functioning, as have been observed in many laboratory and mesocosm experiments (Nisumaa et al., 2010). Common responses are deleterious effects of ocean acidification on calcium carbonate production by marine calcifying phytoplankton (Riebesell et al., 2000; Delille et al., 2005; Ridgwell et al., 2009; Lohbeck et al., 2012) and organisms at higher trophic levels (e.g. Comeau et al. 2009; Lischka et al., 2011). Increasing ambient inorganic carbon concentrations have also been shown to enhance primary production and carbon assimilation in various photoautotrophs, including seagrasses (Palacios and Zimmerman, 2007; Hall-Spencer et al., 2008) and freshwater and marine phytoplankton (Hein and Sand-Jensen, 1997; Schippers et al., 2004; Levitan et al., 2007; Riebesell et al., 2007; Engel et al., 2008; Tortell et al., 2008).

Increasing carbon assimilation by marine phytoplankton could cause a shift in pelagic ecosystems towards higher carbon-to-nutrient utilization ratios (Riebesell et al., 2007; Bellerby et al., 2008). Model studies show that by consuming more carbon in the surface layer, marine phytoplankton may potentially increase the oceanic sink of CO_2 (Schneider et al., 2004). However, the Arctic Ocean is characterized by high heterotrophic bacterioplankton concentrations (Li et al., 2009) leading to net heterotrophy, which is responsible for the rapid turnover of carbon through a highly efficient microbial loop (Rokkan Iversen and Seuthe, 2011; Tremblay et al., 2012).

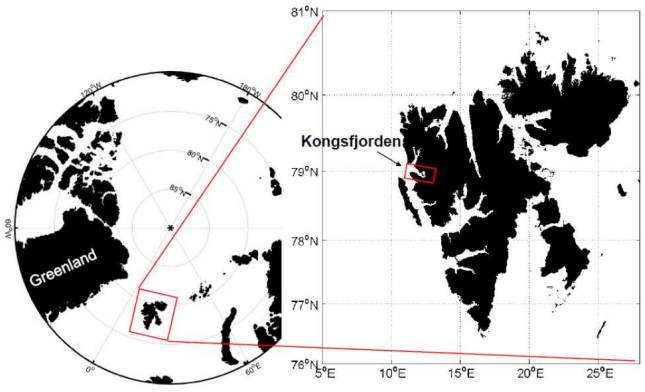

Fig. 1. Map of the Arctic Ocean with the Svalbard archipelago highlighted in red and enlarged map of the latter with a red square indicating the location of Kongsfjorden.

Despite Arctic marine ecosystems experiencing the strongest ocean acidification, no specific ocean acidification mesocosm study has been conducted in the northern high latitudes. This study presents results from the first large-scale pelagic ocean acidification mesocosm experiment conducted in the Arctic. The aim of this work is to investigate the effect of increased pCO_2 on net community production – the balance between CO_2 assimilation due to photosynthesis by autotrophs and CO_2 release due to organic matter respiration by autotrophs and heterotrophs – and net community stoichiometry.

2 Material and methods

2.1 Study area

The mesocosm experiment was performed in Kongsfjorden (78°56.2′ N, 11°53.6′ E, Fig. 1), on the west coast of Spitsbergen, Svalbard archipelago. The water in Kongsfjorden is a mixture of Arctic water masses (which are transported by the coastal current flowing from the Barents Sea over the West Spitsbergen Shelf), Atlantic water masses (West Spitsbergen Current), and freshwater input from melting glaciers and precipitation (Cottier et al., 2005). In winter the hydrography is dominated by Arctic water masses and in summer it is under Atlantic influence (Svendsen et al., 2002).

2.2 Experimental set-up

Nine mesocosm bags two metres in diameter and 17 m long were deployed in Kongsfjorden in late May of 2010. The bags, attached to hard floating frames, were made of thermoplastic polyurethane (TPU). Each mesocosms enclosed 43.9–47.6 m^3 of fjord water (Schulz et al., 2013; Czerny et al., 2013a). Closing the mesocosms at the bottom isolated the interior waters assuring there was no further exchange with the fjord water. Above the bottom plate inside each mesocosm

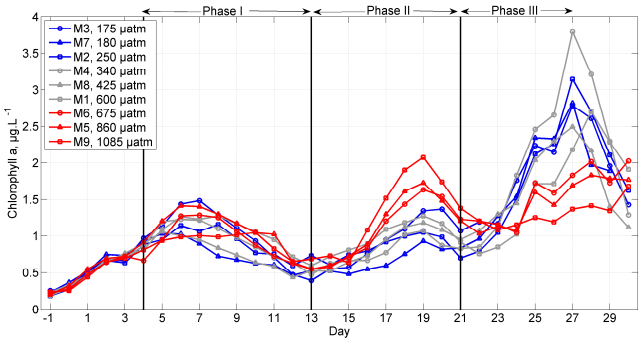

Fig. 2. Temporal evolution of chlorophyll *a* concentrations in different mesocosms. Vertical lines on t_4, t_{13} and t_{22} show the start and the end of each experimental phase. Blue colour of the lines indicates low pCO_2 level, grey – intermediate pCO_2 level and red – high pCO_2 level. Numbers in a legend next to every line with symbol are the rounded pCO_2 levels for t_8–t_{27} period.

was a cone of a sediment trap (see Czerny et al., 2013c, Fig. 1a), which separated the main water column and water below the cone. The water below the cone was not directly manipulated, and had a slow exchange with the main water column. This space below the cone was approximately 8 % of the total enclosures' volume (Riebesell et al., 2013), and is called hereafter "dead volume" (Czerny et al., 2013b). On top of each floating frame there was a hood made of transparent polyvinyl chloride (PVC) to minimize precipitation and external sources of particulate carbon and nitrogen (e.g. aeolian supply and bird excrement) to the mesocosms.

The experiment lasted for 31 days from 7 June (day t_0) to 7 July (day t_{30}). CO_2 addition was implemented in four steps (Schulz et al., 2013). Filtered seawater, enriched with CO_2 was injected into the mesocosms and evenly distributed throughout the water column. Exchange of CO_2-enriched water with unperturbed water in the dead volume caused an initial abrupt decline in pCO_2 levels from day t_4 until day t_8. Therefore pCO_2 levels on t_8 were used as initial values ranging in the different mesocosms from 185 to 1420 µatm. Table 1 shows mean pCO_2 and pH_T values in seven perturbed (M1, M2, M4, M5, M6, M8, M9) and two control mesocosms (M3, M7) for different periods of the experiment, defined according to temporal changes in chlorophyll *a* concentrations (Riebesell et al., 2013): phase I, end of CO_2 manipulation until nutrient addition (t_5–t_{12}), phase II, nutrient addition until 2nd chlorophyll minimum(t_{13}–t_{21}), and phase III, 2nd chlorophyll minimum until end of the experiment (t_{22}–t_{30}). However, the variables for calculating NCP (net community production), C : N and C : P uptake ratios are only available from t_8 onwards, when the perturbed water column had exchanged with the dead volume, and only until t_{27} due to logistical constraints. Therefore, in this study, phase I was defined as t_8–t_{12} and phase III as t_{22}–t_{27}. In addition we evaluated C : N and C : P uptake ratios in the post-nutrient period t_{14}–t_{27} (phase II + phase III).

Nutrients, (5 µM of nitrate (NO_3^-), 0.31 µM of phosphate (PO_4^{3-}), and 2.5 µM of silicate ($Si(OH)_4$)), were added to the mesocosms on day t_{13} to simulate the upwelling of nutrient rich deep waters to the surface (Schulz et al., 2013).

Water samples were collected daily using a 5 L depth-integrated sampler lowered down to 12 m. A more detailed description of the experimental set-up can be found in Riebesell et al. (2013), Czerny et al. (2013a, b, c), and Schulz et al. (2013).

2.3 Data

Concurrent with sampling for other biogeochemical and biological variables, seawater samples for determining the carbon dioxide system were taken daily from the integrated water sampler. Samples for total alkalinity (A_T) and total dissolved inorganic carbon (C_T) were drawn into 500ml borosilicate bottles. No filtering of samples prior to analysis was done due to the lack of significant calcifying plankton (Schulz et al., 2013; Brussaard et al., 2013; Niehoff et al., 2013). A_T was measured using Gran potentiometric titration (Gran, 1952) on a VINDTA system (Mintrop et al., 2000) with a precision of 2 µmol kg^{-1}. C_T was determined using coulometric titration (Johnson et al., 1987) with a precision of $\leq$ 2 µmol kg^{-1}. Measurements for both C_T and A_T were calibrated against certified reference material and values adjusted according to the offsets for each measurement series (CRM; Batch No. 101, http://cdiac.esd.ornl.gov/oceans/Dickson_CRM/rmdata/Batch101.pdf).

CO_2 system calculations

The measured C_T and A_T, with associated temperatures, salinity and dissolved nutrient data, were applied to the CO2SYS program for Matlab (van Heuven et al., 2011) to calculate additional carbon dioxide system variables. To be consistent with Bellerby et al. (2008), we used the dissociation constants for carbonic acid of Dickson and Millero (1987), boric acid from Dickson (1990a), sulphuric acid following Dickson (1990b) and the CO_2 solubility coefficients from Weiss (1974). Values are reported as in situ concentrations. Seawater pH is reported on the total hydrogen scale (pH_T) and pCO_2 in µatm.

To estimate NCP and the stoichiometric rates of carbon to nutrient uptake, we used measurements of total inorganic carbon concentration (C_T), total alkalinity (A_T), inorganic nutrient concentrations (phosphate – PO_4^{3-}, nitrate – NO_3^-, nitrite – NO_2^-, and ammonium – NH_4^+) (Schulz et al., 2013) and air/sea CO_2 gas exchange ($CO_{2(ex.)}$), estimated by measured loss of N_2O added to the mesocosms as a deliberate tracer (Czerny et al., 2013b). We also show the temporal evolution of chlorophyll *a* concentrations (Fig. 2), measured using HPLC according to Welschmeyer (1994) (Schulz et al., 2013).

Table 1. Mean values of pCO_2 and pH_T (total scale) levels in mesocosms for every phase, post-nutrients period t_{14}–t_{27} and the overall period t_8–t_{27}. pCO_2 and pH_T are calculated from total carbon and total alkalinity using CO2SYS for Matlab (van Heuven et al., 2011) . The dissociation constant for carbonic acid was adopted from Dickson and Millero (1987), for boric acid from Dickson (1990a), for sulfuric acid from Dickson (1990b); CO_2 solubility coefficient was adopted from Weiss (1974).

	phase I		phase II		phase III		phase II + phase III		t_8–t_{27}	
	pH_T	pCO_2 (µatm)	pH_T	pCO_2 (µatm)	pH_T	pCO_2 (µatm)	pH_T	pCO_2 (µatm)	pH_T	pCO_2 (µatm)
M3	8.33	185	8.34	176	8.35	170	8.34	174	8.34	177
M7	8.32	187	8.33	179	8.35	170	8.34	175	8.33	179
M2	8.18	270	8.20	253	8.24	233	8.22	245	8.21	252
M4	8.06	375	8.09	344	8.13	309	8.10	329	8.09	342
M8	7.96	480	8.01	422	8.04	389	8.02	409	8.01	426
M1	7.82	690	7.87	594	7.92	533	7.89	568	7.87	598
M6	7.74	820	7.82	665	7.89	578	7.85	629	7.82	676
M5	7.64	1050	7.73	838	7.78	746	7.75	800	7.72	861
M9	7.52	1420	7.64	1033	7.71	891	7.67	974	7.63	1084

Table 2. The results of the F test on linear regressions between NCP, C : N, C : P uptake ratios in different phases and the mean pCO_2 for the corresponding phase.

	Period	Slope	R^2	p
NCP	phase I	0.007	0.849	< 0.001
	phase II	0.007	0.367	0.084
	phase III	−0.029	0.902	< 0.001
	t_8–t_{27}	−0.010	0.348	0.094
C : N ratio	phase II + phase III	−0.004	0.757	0.002
	phase II	0.000	0.001	0.952
	phase III	−0.008	0.409	0.064
C : P ratio	phase II + Phase III	−0.073	0.739	0.003
	phase II	−0.005	0.044	0.588
	phase III	0.219	0.379	0.078

2.4 Net community production derived from changes in C_T concentration

To estimate the net effect of C_T uptake by phytoplankton during photosynthesis and C_T release due to auto- and heterotrophic respiration, we calculated NCP with a method previously employed in the PeECE mesocosm studies (Delille et al., 2005; Bellerby et al., 2008).

A_T was corrected to cumulative changes in inorganic nutrient concentrations (Eq. 1), as for each mole of NO_3^-, NO_2^- and PO_4^{3-} consumed through biosynthesis, total alkalinity increases by 1 mole (Brewer and Goldman, 1976). Additionally, each mole of consumed NH_4^+ decreases total alkalinity by 1 mole (Wolf-Gladrow et al., 2007).

$$A_{T\,\mathrm{corrected}} = A_{T\,\mathrm{measured}} - \Delta NO_3^- - \Delta PO_4^{3-} - \Delta NO_2^- + \Delta NH_4^+ \quad (1)$$

The incremental change in C_T concentration was corrected for the CO_2 air/sea gas exchange (Eq. 2).

$$C_{T\,\mathrm{corrected}} = C_{T\,\mathrm{measured}} - CO_{2(\mathrm{ex.})} \quad (2)$$

Corrected A_T and C_T concentrations were normalized to salinity to account for evaporation from the first day of every phase (Eqs. 3, 4) (Schulz et al., 2013).

$$A_{T\,\mathrm{norm.}}(x_n) = A_{T\,\mathrm{corrected}}(x_n)\,\frac{S(x_n)}{S(x_1)} \quad (3)$$

$$C_{T\,\mathrm{norm.}}(x_n) = C_{T\,\mathrm{corrected}}(x_n)\,\frac{S(x_n)}{S(x_1)}, \quad (4)$$

where, S is salinity, x_n and x_1 correspond to day n and day 1, respectively, of the time period for which A_T and C_T are normalized.

Net community calcification (NCC) was estimated as cumulative change in $A_{T\,\mathrm{norm.}}$ (Eq. 5):

$$\mathrm{NCC} = -0.5\,\frac{\Delta A_{T\,\mathrm{norm.}}}{\Delta t}. \quad (5)$$

Calcification was insignificant during the experiment, therefore calculated NCC expresses the precision of A_T measurements (2 µmol kg^{-1}).

Finally, net community production was computed as the cumulative change in $C_{T\,\mathrm{norm.}}$, accounting for the cumulative change in $A_{T\,\mathrm{norm.}}$ (Eq. 6):

$$\mathrm{NCP} = -\frac{\Delta C_{T\,\mathrm{norm.}}}{\Delta t} + 0.5\,\frac{\Delta A_{T\,\mathrm{norm.}}}{\Delta t}. \quad (6)$$

2.5 Statistical analysis

A gradient of eight CO_2 levels with no replicates allowed for linear regression analysis (Riebesell et al., 2013) in order

Table 3. C : N uptake ratios (Slope), standard deviations (SD) and the results of the F test on linear regression analysis in phases II and III and the post-nutrient period (phase II + phase III) (see explanations in text).

	phase II ($n = 8$)				phase III ($n = 6$)				phase II + phase III ($n = 14$)			
CO_2 level	Slope	SD	R^2	p	Slope	SD	R^2	p	Slope	SD	R^2	p
Low (M3, M2, M7)	4.428	0.437	0.888	< 0.001	15.167	0.394	0.947	0.001	8.889	0.611	0.927	< 0.001
Intermediate (M1, M4, M8)	4.507	0.605	0.960	< 0.001	15.731	2.167	0.935	0.002	8.743	1.104	0.918	< 0.001
High (M5, M6, M9)	4.551	0.745	0.933	< 0.001	13.833	5.311	0.814	0.014	6.581	0.825	0.913	< 0.001

Table 4. C : P uptake ratios, standard deviations and the results of the F test on linear regressions analysis in phases II and III and the post-nutrient period (phase II + phase III) (see explanations in text).

	phase II ($n = 8$)				phase III ($n = 6$)				phase II + phase III ($n = 14$)			
CO_2 level	Slope	SD	R^2	p	Slope	SD	R^2	p	Slope	SD	R^2	p
Low (M3. M2. M7)	62.001	7.730	0.875	0.001	276.242	41.622	0.902	0.004	136.325	18.264	0.892	< 0.001
Intermediate (M1. M4. M8)	54.616	1.618	0.902	< 0.001	290.583	20.009	0.879	0.006	127.303	16.402	0.859	< 0.001
High (M5. M6. M9)	55.317	9.639	0.857	0.001	408.084	123.390	0.596	0.072	92.866	14.426	0.824	< 0.001

to test for the relationship between NCP, and C : N and C : P uptake ratios in each phase and the mean pCO_2 level in the corresponding phase. For the regression analysis we used cumulative NCP on the final day of each phase and C : N and C : P uptake ratios, which were derived from a linear regression described below. The slope of linear regression analysis, R^2 and p values of the F test are shown in Table 2.

A linear regression analysis was performed to define the relationship between NCP in each time period (phase) and the corresponding cumulative change in inorganic nitrogen (ΔN) and phosphorus (ΔP). The cumulative change in inorganic nitrogen resulted from a sum of a cumulative change in nitrate, nitrite and ammonia. The relationships for each time period were defined with an equation type $\Upsilon = \alpha X + \beta$, where coefficient α corresponded to the C : N or C : P uptake ratio. Tables 3 and 4 show averaged coefficients α for low, intermediate and high pCO_2 levels (slope), as well as corresponding standard deviations. All statistical analyses were performed with the Statistics toolbox in Matlab.

3 Results

The initial characterization of the CO_2 system in the mesocosm and the fjord was performed on t_{-3} prior to the CO_2 addition (Riebesell et al., 2013). The initial pCO_2 of the ambient water in the fjord was ~ 170 µatm, corresponding to a pH_T of ~ 8.3. The mesocosm values agreed to ± 1.2 µmol kg^{-1}, i.e. within the measurement precision, for both C_T and A_T. This confirmed that the closing of the bags isolated water of very similar biogeochemical properties in each mesocosm; a significant feat due to the typical small scale heterogeneity of the fjord (Svendsen et al., 2002). Following the final carbon dioxide perturbations on t_4 (Schulz et al., 2013; Riebesell et al., 2013) it took a further four days for the CO_2 system to settle down in the mesocosms due to slow exchange with dead volume in the base of the bags and thus, all changes to the CO_2 fields were referenced to t_8. A phytoplankton bloom developed in the mesocosm (Schulz et al., 2013) and CO_2 was drawn down due to high primary productivity (Engel et al., 2013). Primary production (Engel et al., 2013) showed significant sensitivity to the initial and bloom phase CO_2 conditions. A breakdown of the CO_2 sensitivity on the development of the particulate and dissolved elemental pools is described in Czerny et al. (2013c).

The daily measurements of the measured carbonate system variables (C_T and A_T) and the calculated variables (pCO_2, pH_T and Ω_{ar}) for all mesocosms and the background fjord values are shown in Fig. 3. The net changes in these variables, relative to t_8, are illustrated in Fig. 4.

Total alkalinity increased steadily in all the bags from 2242 on t_8 to 2247 µmol kg^{-1} on t_{25} falling back to the original 2242 µmol kg^{-1} by t_{27} (Figs. 3, 4). The increase was due to freshwater losses, following evaporation, and nutrient uptake as, in the absence of significant numbers of calcifiers (Schulz et al., 2013; Brussaard et al., 2013; Niehoff et al., 2013), there were no significant A_T changes due to calcification. The effect of nutrient addition on t_{13} could not be seen in A_T as the addition was alkalinity neutral due to the concomitant addition of acid (Riebesell et al., 2013). As there were no other changes in other associated biogeochemical variables and salinity, it is likely that the drop in A_T on t_{27} was a calibration offset.

C_T concentrations showed high variability between the mesocosms in response to the deliberate additions of CO_2 (Figs. 3, 4). From an original fjord value of about 1982 µmol kg^{-1}, the perturbations spanned a range from 1982 to 2270 µmol kg^{-1}. In the high CO_2 scenarios, C_T drops rapidly and consistently throughout the experiment with net C_T changes between 52 and 63 µmol kg^{-1}. In the

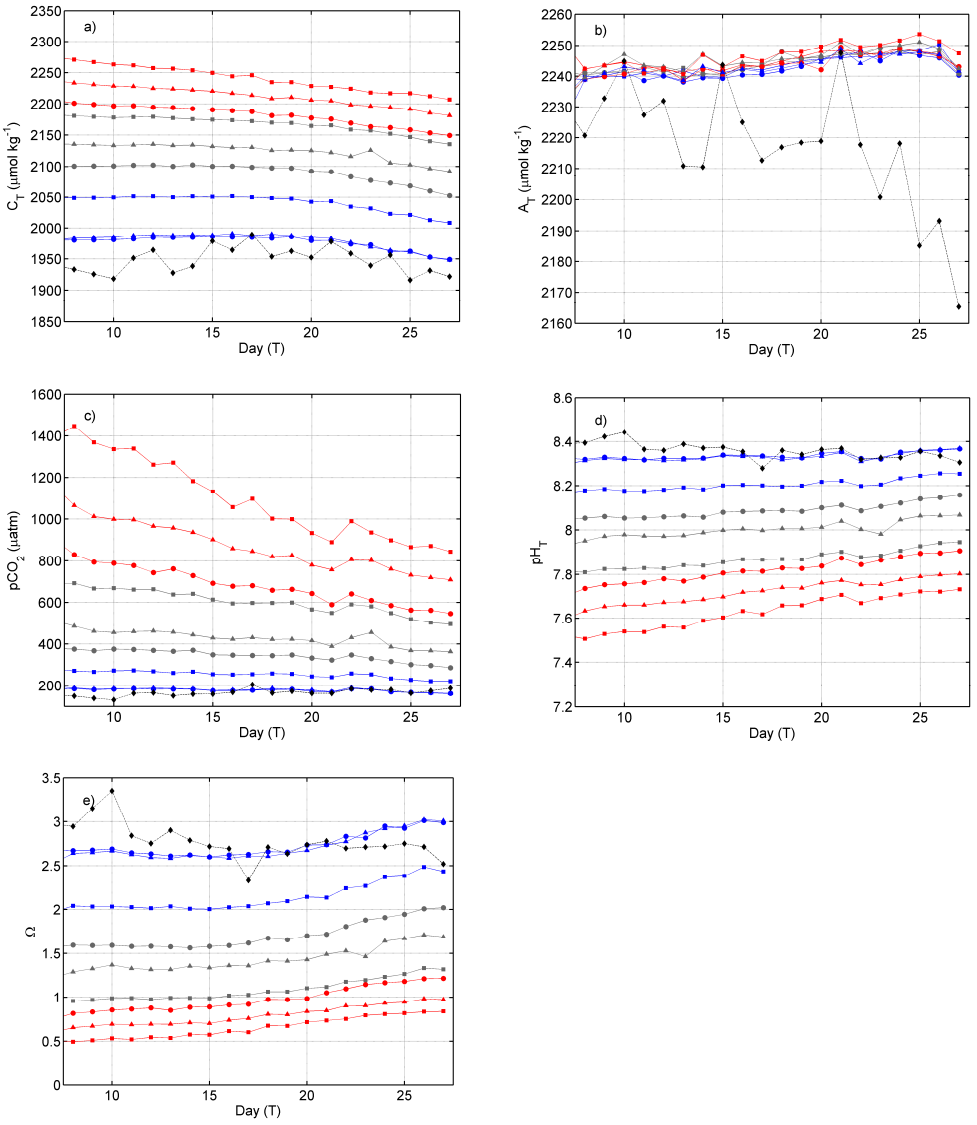

Fig. 3. Absolute values for the marine carbonate system variables. Measured values are **(a)** total inorganic carbon (C_T) and **(b)** total alkalinity (A_T). Calculated values are **(c)** partial pressure of carbon dioxide (pCO_2), **(d)** pH_T on the total hydrogen scale and **(e)** aragonite saturation state (Ω_{ar}). Red symbols: high pCO_2 mesocosms (M5, M6, M9), grey symbols: medium pCO_2 mesocosms (M1, M4, M8), blue symbols: low pCO_2 mesocosms (M2, M3, M7). The black line represents the natural fjord background variability.

intermediate CO_2 scenarios, C_T concentrations change much more slowly until about t_{23} after which there is a much faster reduction. Total reductions in the intermediate scenario were between 54 and 58 µmol kg^{-1}. In the low CO_2 scenario mesocosms, C_T increases until t_{19} before exhibiting the fastest decline of all the scenarios towards the end of the experiment resulting in a net change of between 31 and 40 µmol kg^{-1}.

The initial mesocosm pCO_2 concentrations were chosen to represent a range of atmospheric values corresponding to anticipated carbon fossil fuel release scenarios. pCO_2 showed very large inter- and intra-mesocosm variability, particularly in the high CO_2 scenarios (Figs. 3, 4). This is due to the poor buffer capacity of the seawater that results in increasing sensitivity in pCO_2 to even small changes in C_T and A_T that result from both net ecosystem perturbations and from measurement sensitivity. The higher CO_2 scenario mesocosms also exhibited the largest reductions in pCO_2 enhanced by rapid exchange with the atmosphere (Czerny et al., 2013b).

Initial pH_T levels ranged from 7.5 to 8.3 and, in all bags, increased through the experiments according to the relative amounts of CO_2 exchange with the overlying atmosphere and biological net carbon production (Figs. 3, 4). The high CO_2 mesocosm exhibited the greatest pH_T changes.

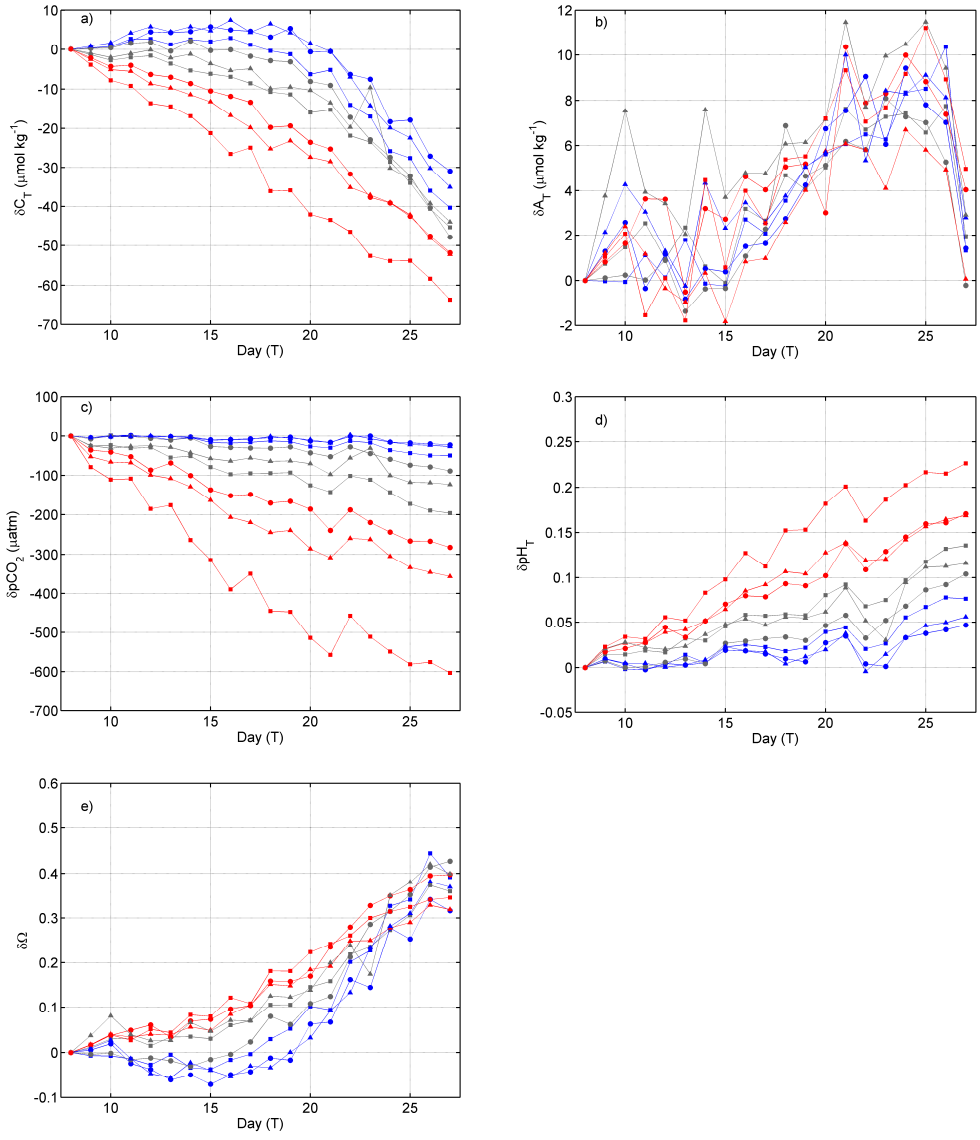

Fig. 4. Cumulative changes relative to the start of the post CO_2 perturbation (t_8). **(a)** total inorganic carbon (C_T), **(b)** total alkalinity (A_T), **(c)** partial pressure of carbon dioxide (pCO_2), **(d)** pH_T on the total hydrogen scale and **(e)** aragonite saturation state (Ω_{ar}). Red symbols: high pCO_2 mesocosms (M5, M6, M9), grey symbols: medium pCO_2 mesocosms (M1, M4, M8), blue symbols: low pCO_2 mesocosms (M2, M3, M7). The black line represents the natural fjord background variability.

The aragonite saturation state (Ω_{ar}) displayed the highest values (2.6) in the control mesocosms (Fig. 3). The seawater was undersaturated with respect to aragonite in the four highest CO_2 mesocosms with the lowest Ω_{ar} of the experiment being 0.5. Seawater was undersaturated with respect to aragonite for the entire experimental period under the highest CO_2 scenario (Fig. 3).

Concentrations of nitrate and phosphate in the water were close to detection limit at the beginning of the experiment (0.11 µmol kg^{-1} for nitrate, 0.13 µmol kg^{-1} for phosphate). Concentration of ammonia was 0.7 µmol kg^{-1} (Schulz et al., 2013). Additionally, there were 5.5 µmolkg^{-1} of dissolved organic nitrogen, 0.20 µmol kg^{-1} of dissolved organic phosphorus (Schulz et al., 2013) and 75 µmol kg^{-1} of dissolved organic carbon (Engel et al., 2013). A post-bloom situation in the fjord at the start of the experiment was identified.

Despite relatively low nutrient concentrations chlorophyll *a* increased steadily from 0.2 µg L^{-1} at day t_3 to 1.4 µg L^{-1} at days t_6–t_8 (Fig. 2; Schulz et al., 2013). After day t_8 chlorophyll *a* declined reaching minimum concentrations on day t_{13}. Addition of mineral nutrients on day t_{13} stimulated phytoplankton biomass with Chl *a* peaking on day t_{19} at 2 µg L^{-1} in the highest CO_2 treatment and a minimum of 1 µg L^{-1} in one of the control mesocosms

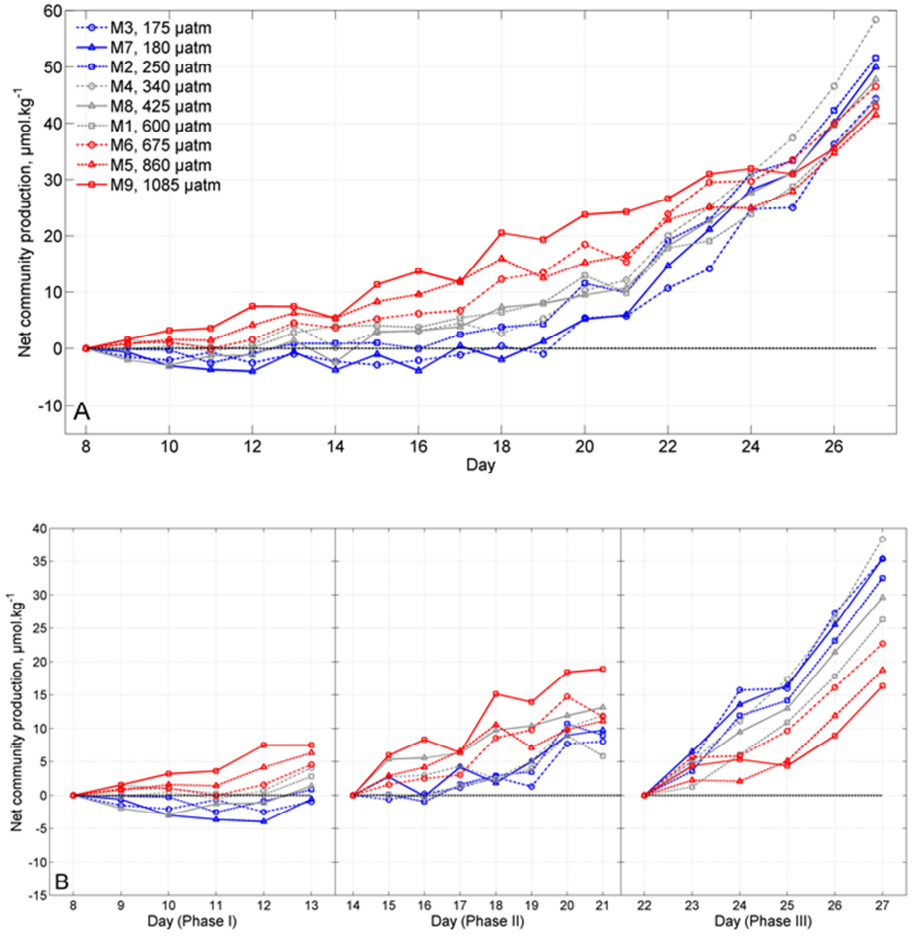

Fig. 5. (A) Net community production for the total period of the experiment; **(B)** net community production in every phase of the experiment. Horizontal dashed line on both figures shows the border between heterotrophic (below 0) and autotrophic (above 0) systems. Line colours and numbers in a legend are as described for Fig. 2.

(Schulz et al., 2013). After the second minimum on day t_{21}, chlorophyll *a* increased in low and intermediate CO_2 treatments, peaking on day t_{27} with values of 2.5–3.7 µg L^{-1}. In the high CO_2 treatment, chlorophyll *a* concentration increased gradually towards the end of the experiment, yet did not exceed 2 µg L^{-1}. The phytoplankton community was composed predominantly of haptophytes in phase I, prasinophytes, dinoflagellates, and cryptophytes in phase II, haptophytes, prasinophytes, dinoflagellates and chlorophytes in phase III (Schulz et al., 2013). There was also significant plankton wall growth that built up during the experiment (Czerny et al., 2013c).

Cumulative NCP was similar in all mesocosms, reaching 50.0 ± 5.0 µmol kg^{-1} by day t_{27} (Fig. 5a). In phase I, NCP was positive in the high and intermediate CO_2 treatments accounting for 6.1 ± 1.5 and 2.8 ± 1.4 µmol kg^{-1}, respectively (Figs. 5b, 6), indicating a net autotrophic system. NCP in mesocosms with low CO_2 treatments was close to zero (-0.2 ± 0.9 µmol kg^{-1}), indicating that autotrophic and heterotrophic processes were in balance. In phase II, NCP was positive and higher than in phase I in all mesocosms. The highest NCP was in the high CO_2 treatments, on average 13.9 ± 4.3 µmol kg^{-1} with the intermediate and low CO_2 treatments having 10.3 ± 3.9 and 8.9 ± 0.9 µmol kg^{-1}, respectively. In phase III NCP was highest of all the phases for all scenarios. The highest NCP was in the low (34.4 ± 1.7 µmol kg^{-1}) and intermediate CO_2 treatments (31.4 ± 6.2 µmol kg^{-1}), while in the high CO_2 treatments NCP was 19.2 ± 3.2 µmol kg^{-1}. NCP showed a significant positive linear relationship with increasing pCO_2 levels in phase I ($p < 0.001$) (Table 2), but significant negative linear relationship with increasing pCO_2 levels in phase III ($p < 0.001$).

Due to the very low concentrations of inorganic nutrients in phase I, around the limit of detection (Fig. 6) calculations of stoichiometric uptake rates provided unreasonable values. Therefore, we evaluated the cumulative changes in inorganic nutrients, C : N and C : P uptake ratios for phase II, III and phase II + III only. By the end of phase II, the cumulative change in

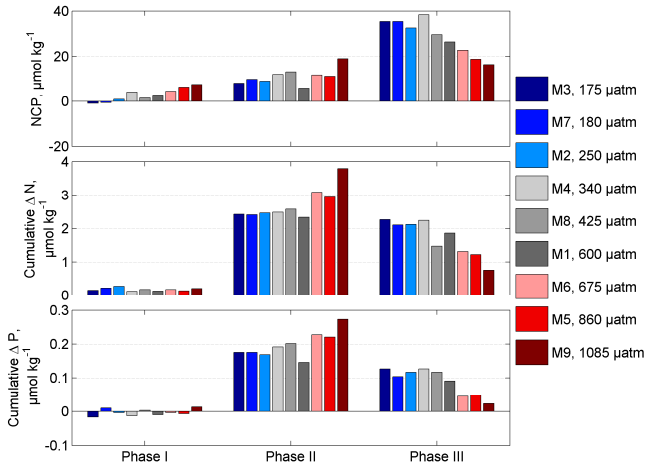

Fig. 6. Net community production, cumulative change in inorganic nitrogen (ΔN) and cumulative change in inorganic phosphorus (ΔP) on the last day of every experimental phase for 9 mesocosms.

inorganic nitrogen was on average $2.43 \pm 0.03\,\mu mol\,kg^{-1}$ in the low, $2.47 \pm 0.13\,\mu mol\,kg^{-1}$ in the intermediate and $3.27 \pm 0.50\,\mu mol\,kg^{-1}$ in the high CO_2 treatments (Fig. 6). The cumulative change in inorganic phosphorous was $0.17 \pm 0.04\,\mu mol\,kg^{-1}$ in the low, $0.18 \pm 0.03\,\mu mol\,kg^{-1}$ in the intermediate and $0.24 \pm 0.03\,\mu mol\,kg^{-1}$ in the high CO_2 treatments. In phase III, the cumulative change in inorganic nitrogen was on average $2.16 \pm 0.09\,\mu mol\,kg^{-1}$ in the low, $1.86 \pm 0.38\,\mu mol\,kg^{-1}$ in the intermediate and $1.09 \pm 0.30\,\mu mol\,kg^{-1}$ in the high CO_2 treatments. The corresponding change in inorganic phosphorus was $0.12 \pm 0.01\,\mu mol\,kg^{-1}$ in the low, $0.11 \pm 0.02\,\mu mol\,kg^{-1}$ in the intermediate and only $0.04 \pm 0.02\,\mu mol\,kg^{-1}$ in the high CO_2 treatments (Fig. 6). In contrast to phase II, the amount of inorganic nitrogen and phosphorus consumed by the community in phase III was lower at high CO_2 in comparison to intermediate and low CO_2 levels. This was primarily due to the high nutrient consumption in phase II that resulted in rapid nutrient depletion under high CO_2 in phase III.

In phase II C : N and C : P uptake ratios were similar in all mesocosms and lower than respective Redfield ratios. (Tables 3, 4 and Fig. 7) In phase III, C : N and C : P were higher than respective Redfield ratios, probably due to very low concentrations of inorganic nutrients available at the end of phase III (Fig. 7b, d). C : N and C : P were slightly lower in the high CO_2 in comparison to the intermediate and low CO_2 treatments (Fig. 7b, Table 3). Combining phase II and III, C : N and C : P uptake ratios were close to the respective Redfield ratios and C : N uptake ratios decreased with increasing pCO_2 from 8.9 ± 0.6 in the low and 8.7 ± 1.1 in the intermediate to 6.6 ± 0.8 in the high pCO_2 treatments (Table 3). In a similar manner, C : P uptake ratios also decreased with increasing pCO_2 from 136.3 ± 18.3 in the low and 127.3 ± 16.4 in the intermediate to 92.8 ± 14.4 in the high pCO_2 treatments (Table 4). This trend, based on averages, was confirmed by linear regression analyses taking into account individual CO_2 levels in each mesocosm, and was found to be statistically significant (Table 2).

4 Discussion

NCP increased with increasing pCO_2 in phase I, which was consistent with the higher growth of small-sized phytoplankton (0.8–2.0 µm) stimulated by elevated CO_2 (Brussaard et al., 2013). The inherited fjord water had low autotrophic production. The initial concentrations of inorganic nutrients in the mesocosms on t_0, suggested Si limitation for Si-consuming phytoplankton, and N deficient for the other phytoplankton. Such a situation may have promoted the growth of pico- and nanophytoplankton with low or absent silicate demand and they could have had a competitive advantage under low nutrient concentration during phase I. Remineralization of inorganic nutrients from organic matter indicates that in a post-bloom situation in Kongsfjorden at the very start of the experiment only very slightly net-heterotrophic (Rokkan Iversen and Seuthe, 2011; de Kluijver et al., 2013). Mixotrophy could also have contributed to the phase I balance. Large zooplankton abundance was high (Niehoff et al., 2013) and would have contributed to the remineralization of organic matter. Balanced to moderately positive NCP in phase I was fuelled by phosphate remineralized from organic matter and most importantly ammonia as an N source (Schulz et al., 2013). In mesocosms with intermediate and high pCO_2, NCP was positive, indicating that production rates were higher than respiration rates, and most likely the phytoplankton were mildly stimulated by elevated CO_2 (Engel et al., 2013). However, the effect size is small and positive NCP could also be caused by relatively low respiration rates in the high CO_2 treatments, as there was increased sedimentation of freshly produced organic matter with increasing CO_2 (de Kluijver et al., 2013). Zooplankton grazing decreased from low to high pCO_2 treatment (de Kluijver et al., 2013) and thus could also contribute to the NCP increase with increasing pCO_2. However, the dominant cause of the high NCP to increased CO_2 was higher exudation of DOC (dissolved organic carbon; Engel et al, 2013; Czerny et al. 2013c).

Phytoplankton growth in phase I was terminated by viral infection (Brussaard et al., 2013), but after nutrient addition at the beginning of phase II, phytoplankton numbers started to rise showing increasing growth rates with higher pCO_2 (Brussaard et al., 2013; Schulz et al., 2013). Following phytoplankton growth, NCP was positive in phase II, indicating net autotrophy in all mesocosms. Higher rates of NCP with increasing pCO_2 show that small-sized phytoplankton, which was dominant in phase II (Brussaard et al., 2013; Schulz et al., 2013), fixed more dissolved inorganic carbon at higher CO_2 levels. Along with inorganic carbon

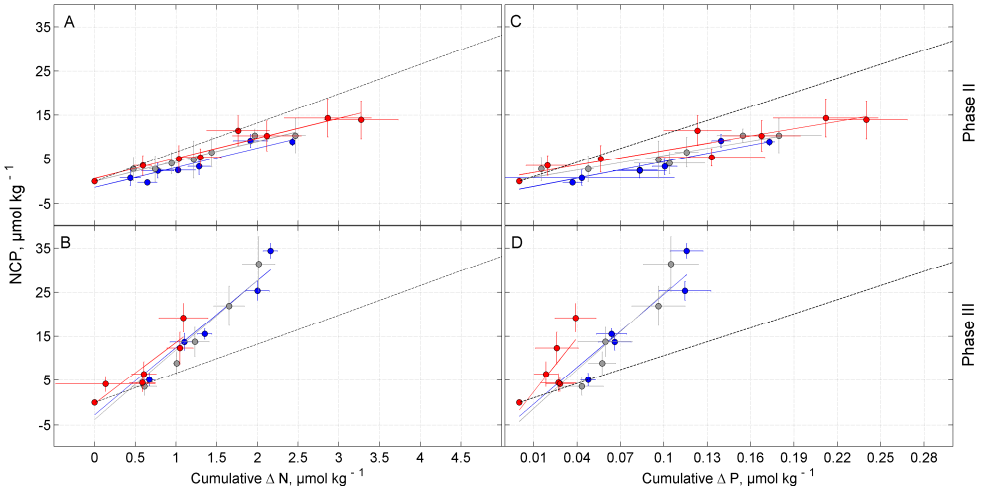

Fig. 7. Ratios of net community production to a cumulative change in inorganic nitrogen **(A)** and phosphorus **(C)** in phase II and phase III **(B)**, **(D)** (C : N and C : P uptake ratios). Data and slopes are averaged for low (blue), intermediate (grey) and high (red) pCO_2 treatment. Error bars are 1 standard deviation. Slopes were calculated with linear regression analysis (see Methods section for details). Slopes of linear regression analysis and statistics of the F test are shown in Table 3 for C : N uptake ratio and in Table 4 for C : P uptake ratio. Dashed black lines are the Redfield C : N and C : P elemental ratios.

there was also greater utilization of inorganic nutrients in the high pCO_2 treatments (Schulz et al., 2013). Increased NCP at high CO_2 was reflected by high concentrations of particulate organic carbon (POC) (Schulz et al., 2013). Nutrient addition also stimulated the production of DOC, which increased with increasing pCO_2 (Engel et al., 2013). Concentrations of DOC, however, did not change significantly after nutrient addition, indicating higher DOC consumption by bacteria with increasing pCO_2 (Engel et al., 2013). Like phytoplankton, bacteria require inorganic nutrients to grow and to increase their biomass (Thingstad et al., 2008), thus higher abundance of both phytoplankton and bacteria in mesocosms with high pCO_2 results in an increased demand for mineral nutrients. Phytoplankton growth in phase II was again terminated by viral infection (Brussaard et al., 2013).

NCP rates in phase III were the highest of the phases of the experiment. There was a greater abundance of large phytoplankton during the bloom in phase III than in earlier phases (Brussaard et al., 2013). The negative effect of elevated CO_2 on phytoplankton growth and NCP rates in phase III should not be interpreted as a CO_2-response but was due to nutrient limitation following the high biomass accumulation in phase II. Production of dissolved organics (and increased wall growth) was probably also high during phase III when inorganic nutrients became limiting (Czerny et al, 2013c).

NCP in this investigation was similar to the NCP calculated from ^{13}C labelling (de Kluijver et al., 2013) and to NCP based on changes in dissolved oxygen concentration during light/dark incubations (see comparison analysis by Tanaka et al., 2013). However, NCP estimates did not agree very well with primary production (PP) of POC and DOC based on 24 h ^{14}C incubations, reported in Engel et al. (2013). The mismatch between PP and NCP is a result of the different methodological approaches to determine net carbon uptake. The ^{14}C method measures "new production" over periods of hours, whereas the integrated NCP measures the whole system carbon balance. Most importantly, the PP data of Engel et al. (2013) are derived from single depth incubations (1m) and received about 60 % of incoming light, whereas NCP data captured productivity over the whole mesocosm water column. Moreover, water for the incubations in the study of Engel et al. (2013) was sampled in the mesocosms and prefiltered using 200 µ m meshes. This may have lead to overestimation of phytoplankton productivity in the ^{14}C incubations as grazing by larger zooplankton was excluded.

Stoichiometric uptake ratios, C : N and C : P, evaluated in this study were lower than the respective Redfield ratios in phase II and higher than the respective Redfield ratio in phase III. The phase separation reflects the different biogeochemical demands of the dominant plankton functional types (PFT) and the different life stage biogeochemical requirements. Another source of control on community stoichiometry would have been the nutrient requirements of bacteria, which significantly increased in biomass during the course of the experiment (Brussaard et al., 2013). An efficient recycling system with high bacterial abundance is typical for Kongsfjorden for the post-bloom time of the year (Rokkan-Iversen and Seuthe, 2011). However, a pCO_2-sensitive effect on bacterial respiration was not observed during the experiment (Motegi et al., 2013). Tanaka et al. (2013) also described no pCO_2 effect on community respiration. These findings imply that the role of bacterioplankton as competitor for mineral nutrients could be strengthened in the Arctic Ocean (Thingstad et al., 2008),

while their role in recycling organic matter into inorganic carbon and nutrients could remain unchanged.

The complexity of the results from this experiment challenges any delivery of any simple mathematical representations of the Arctic pelagic ecosystem NCP and nutrient uptake response to a high CO_2 world. Further work is required on Arctic plankton to investigate individual PFT responses and changes to species interaction under ocean acidification. This experiment identifies the importance of studying collectively the interactions of autotrophic, mixotrophic and heterotrophic components if we are to untangle the complexities of future marine ecosystem change. Experiments are also required over all seasons and it should be emphasized that the experiment was performed after the first natural spring bloom had passed and thus the nutrient perturbation, although potentially simulating fresh nutrient supply from, for example, a storm event, was likely to generate responses which cannot readily be applied to the entire growth season. It is important to keep this in mind if extrapolating these results to future changes in the Arctic Ocean.

Acknowledgements. This work is a contribution to the "European Project on Ocean Acidification" (EPOCA) which received funding from the European Community's Seventh Framework Programme (FP7/2007–2013) under grant agreement No. 211384. This work was partially funded by the project Marine Ecosystem Response to a Changing Climate (MERCLIM No. 184860) financed by the program NORKLIMA through the Norwegian Research Council, "Marine Ecosystem Evolution in a Changing Environment" (MEECE No. 212085) and "Basin-scale Analysis, Synthesis and Integration" (EURO-BASIN No. 26493). We gratefully acknowledge the logistical support of Greenpeace International for its assistance with the transport of the mesocosm facility from Kiel to Ny-Ålesund and back to Kiel. We also thank the captains and crews of M/V *ESPERANZA* of Greenpeace and R/V *Viking Explorer* of the University Centre in Svalbard (UNIS) for assistance during mesocosm transport and during deployment and recovery in Kongsfjorden. We thank the staff of the French–German Arctic Research Base at Ny-Ålesund, in particular Marcus Schumacher, for on-site logistical support. Siv Lauvset, Camille Li, Mathias Trachsel and Alexey Pavlov are thanked for providing feedback on an earlier version of this manuscript. This is publication number A425 of the Bjerknes Centre for Climate Research.

Edited by: J. Middelburg

References

Anderson, L. G., Tanhua, T., Bjork, G., Hjalmarsson, S., Jones, E. P., Jutterstrom, S., Rudels, B., Swift, J. H., and Wahlstom, I.: Arctic ocean shelf-basin interaction: An active continental shelf CO_2 pump and its impact on the degree of calcium carbonate solubility, Deep-Sea Res. Pt. I, 57, 869–879, doi:10.1016/j.dsr.2010.03.012, 2010.

Arrigo, K. R., van Dijken, G., and Pabi, S.: Impact of a shrinking Arctic ice cover on marine primary production, Geophys. Res. Lett., 35, L19603, doi:10.1029/2008gl035028, 2008.

Bates, N. R., Orchowska, M. I., Garley, R., and Mathis, J. T.: Seasonal calcium carbonate undersaturation in shelf waters of the Western Arctic Ocean; how biological processes exacerbate the impact of ocean acidification, Biogeosciences Discuss., 9, 14255–14290, doi:10.5194/bgd-9-14255-2012, 2012.

Bellerby, R. G. J., Olsen, A., Furevik, T., and Anderson, L. A.: Response of the surface ocean CO2 system in the Nordic Seas and North Atlantic to climate change, in: Climate Variability in the Nordic Seas, edited by: Drange, H., Dokken, T. M., and Furevik, T., Geophys. Monogr. Ser., AGU, 189–198, 2005.

Bellerby, R. G. J., Schulz, K. G., Riebesell, U., Neill, C., Nondal, G., Heegaard, E., Johannessen, T., and Brown, K. R.: Marine ecosystem community carbon and nutrient uptake stoichiometry under varying ocean acidification during the PeECE III experiment, Biogeosciences, 5, 1517–1527, doi:10.5194/bg-5-1517-2008, 2008.

Brewer, P. G. and Goldman, J. C.: Alkalinity changes generated by phytoplankton growth, Limnol. Oceanogr., 21, 108–117, 1976.

Brussaard, C. P. D., Noordeloos, A. A. M., Witte, H., Collenteur, M. C. J., Schulz, K., Ludwig, A., and Riebesell, U.: Arctic microbial community dynamics influenced by elevated CO_2 levels, Biogeosciences, 10, 719–731, doi:10.5194/bg-10-719-2013, 2013.

Cai, W. J., Chen, L., Chen, B., Gao, Z., Lee, S. H., Chen, J., Pierrot, D., Sullivan, K., Wang, Y., Hu, X., Huang, W. J., Zhang, Y., Xu, S., Murata, A., Grebmeier, J. M., Jones, E. P., and Zhang, H.: Decrease in the CO_2 uptake capacity in an ice-free Arctic Ocean basin, Science, 329, 556–559, doi:10.1126/science.1189338, 2010.

Chierici, M. and Fransson, A.: Calcium carbonate saturation in the surface water of the Arctic Ocean: undersaturation in freshwater influenced shelves, Biogeosciences, 6, 2421–2431, doi:10.5194/bg-6-2421-2009, 2009.

Christensen, J. H., Hewitson, B., Busuioc, A., Chen, A., Gao, X., Held, I., Jones, R., Kolli, R. K., Kwon, W.-T., Laprise, R., Magana Rueda, V., Mearns, L., Menéndez, C. G., Råisånen, J., Rinke, A., Sarr, A., and Whetton, P.: Regional climate projections, in: Climate Change 2007: The Physical Science Basis, Contribution of Working Group I to the Fourth Assessment Report of the Intergovernmental Panel on Climate Change, edited by: Solomon, S., Qin, D., Manning, M., Chen, Z., Marquis, M., Averyt, K. B., Tignor, M., and Miller, H. L., Cambridge University Press, Cambridge, United Kingdom and New York, NY, USA, 849–946, 2007.

Comeau, S., Gorsky, G., Jeffree, R., Teyssié, J.-L., and Gattuso, J.-P.: Impact of ocean acidification on a key Arctic pelagic mollusc (Limacina helicina), Biogeosciences, 6, 1877–1882, doi:10.5194/bg-6-1877-2009, 2009.

Cottier, F., Tverberg, V., Inall, M., Svendsen, H., Nilsen, F., and Griffiths, C.: Water mass modification in an Arctic fjord through cross-shelf exchange: the seasonal hydrography of Kongsfjorden, Svalbard, J. Geophys. Res., 110, C12005, doi:10.1029/2004JC002757, 2005.

Czerny, J., Schulz, K. G., Krug, S. A., Ludwig, A., and Riebesell, U.: Technical Note: The determination of enclosed water volume in large flexible-wall mesocosms "KOSMOS", Biogeosciences,

10, 1937–1941, doi:10.5194/bg-10-1937-2013, 2013a.

Czerny, J., Schulz, K. G., Ludwig, A., and Riebesell, U.: Technical Note: A simple method for air–sea gas exchange measurements in mesocosms and its application in carbon budgeting, Biogeosciences, 10, 1379–1390, doi:10.5194/bg-10-1379-2013, 2013b.

Czerny, J., Schulz, K. G., Boxhammer, T., Bellerby, R. G. J., Büdenbender, J., Engel, A., Krug, S. A., Ludwig, A., Nachtigall, K., Nondal, G., Niehoff, B., Silyakova, A., and Riebesell, U.: Implications of elevated CO_2 on pelagic carbon fluxes in an Arctic mesocosm study – an elemental mass balance approach, Biogeosciences, 10, 3109–3125, doi:10.5194/bg-10-3109-2013, 2013c.

de Kluijver, A., Soetaert, K., Czerny, J., Schulz, K. G., Boxhammer, T., Riebesell, U., and Middelburg, J. J.: A ^{13}Clabelling study on carbon fluxes in Arctic plankton communities under elevated CO_2 levels, Biogeosciences, 10, 1425–1440, doi:10.5194/bg-10-1425-2013, 2013.

Delille, B., Harlay, J., Zondervan, I., Jacquet, S., Chou, L., Wollast, R., Bellerby, R. G. J., Frankignoulle, M., Borges, A. V., Riebesell, U., and Gattuso, J. P.: Response of primary production and calcification to changes of pCO_2 during experimental blooms of the coccolithophoridEmilianiahuxleyi, Global Biogeochem. Cy., 19, GB2023, doi:10.1029/2004gb002318, 2005.

Dickson, A. G.: Thermodynamics of the Dissociation of Boric-Acid in Synthetic Seawater from 273.15-K to 318.15-K, Deep-Sea Res., 37, 755–766, 1990a.

Dickson, A. G.: Standard Potential of the Reaction – Agcl(S) + 1/2h-2(G) = Ag(S) + Hcl(Aq) and the Standard Acidity Constant of the Ion Hso4-K in Synthetic Sea-Water from 273.15-K to 318.15-K, J. Chem. Thermodyn., 22, 113–127, 1990b.

Dickson, A. G. and Millero, F. J.: A Comparison of the Equilibrium-Constants for the Dissociation of Carbonic-Acid in Seawater Media, Deep-Sea Res., 34, 1733–1743, 1987.

Engel, A., Schulz, K. G., Riebesell, U., Bellerby, R., Delille, B., and Schartau, M.: Effects of CO_2 on particle size distribution and phytoplankton abundance during a mesocosm bloom experiment (PeECE II), Biogeosciences, 5, 509–521, doi:10.5194/bg-5-509-2008, 2008

Engel, A., Borchard, C., Piontek, J., Schulz, K. G., Riebesell, U., and Bellerby, R.: CO_2 increases ^{14}C primary production in an Arctic plankton community, Biogeosciences, 10, 1291–1308, doi:10.5194/bg-10-1291-2013, 2013.

Gran, G.: Determination of the equivalence point in potentiometric titrations of seawater with hydrochloric acid, Oceanol. Acta, 5, 209–218, 1952.

Hall-Spencer, J. M., Rodolfo-Metalpa, R., Martin, S., Ransome, E., Fine, M., Turner, S. M., Rowley, S. J., Tedesco, D., and Buia, M. C.: Volcanic carbon dioxide vents show ecosystem effects of ocean acidification, Nature, 454, 96–99, doi:10.1038/nature07051, 2008.

Hein, M., and Sand-Jensen, K.: CO_2 increases oceanic primary production, Nature, 388, 526–527, 1997.

Johnson, K. M., Sieburth, J. M., Williams, P. J., and BrandstrÖm, L.: Coulometric total carbon analysis for marine studies, automation and calibration, Mar. Chem., 21, 117–133, 1987.

Levitan, O., Rosenberg, G., Setlik, I., Setlikova, E., Grigel, J., Klepetar, J., Prasil, O., and Berman-Frank, I.: Elevated CO2enhances nitrogen fixation and growth in the marine cyanobacteriumTrichodesmium, Glob. Change Biol., 13, 531–538, doi:10.1111/j.1365-2486.2006.01314.x, 2007.

Li, W. K. W., McLaughlin, F. A., Lovejoy, C., and Carmack, E. C.: Smallest Algae Thrive As the Arctic Ocean Freshens, Science, 326, p. 539, doi:10.1126/science.1179798, 2009.

Lischka, S., Büdenbender, J., Boxhammer, T., and Riebesell, U.: Impact of ocean acidification and elevated temperatures on early juveniles of the polar shelled pteropod *Limacinahelicina*: mortality, shell degradation, and shell growth, Biogeosciences, 8, 919–932, doi:10.5194/bg-8-919-2011, 2011.

Loeng, H.: Marine systems, in: Arctic Climate Impact Assessment (ACIA), edited by: Symon, C., Arris, L., and Heal, B., Cambridge University Press, New York, 453–538, 2005.

Lohbeck, K. T., Riebesell, U., and Reusch, T. B. H.: Adaptive evolution of a key phytoplankton species to ocean acidification, Nature Geosci., 5, 346–351, doi:10.1038/ngeo1441, 2012.

McPhee, M. G., Proshutinsky, A., Morison, J. H., Steele, M., and Alkire, M. B.: Rapid change in freshwater content of the Arctic Ocean, Geophys. Res. Lett., 36, L10602, doi:10.1029/2009gl037525, 2009.

Mintrop, L., Fernández-Pérez, F., González Dávila, M., Körtzinger, A., and Santana Casiano, J. M.: Alkalinity determination by potentiometry- intercalibration using three different methods, Ciencias Marinas, 26, 23–37, 2000.

Motegi, C., Tanaka, T., Piontek, J., Brussaard, C. P. D., Gattuso, J.-P., and Weinbauer, M. G.: Effect of CO_2 enrichment on bacterial metabolism in an Arctic fjord, Biogeosciences, 10, 3285–3296, doi:10.5194/bg-10-3285-2013, 2013.

Niehoff, B., Schmithüsen, T., Knüppel, N., Daase, M., Czerny, J., and Boxhammer, T.: Mesozooplankton community development at elevated CO_2 concentrations: results from a mesocosm experiment in an Arctic fjord, Biogeosciences, 10, 1391–1406, doi:10.5194/bg-10-1391-2013, 2013.

Nisumaa, A.-M., Pesant, S., Bellerby, R. G. J., Delille, B., Middelburg, J. J., Orr, J. C., Riebesell, U., Tyrrell, T., Wolf-Gladrow, D., and Gattuso, J.-P.: EPOCA/EUR-OCEANS data compilation on the biological and biogeochemical responses to ocean acidification, ESSD, 2, 167–175, doi:10.5194/essd-2-167-2010, 2010.

Palacios, S. L. and Zimmerman, R. C.: Response of eelgrass Zostera marina to CO_2 enrichment: possible impacts of climate change and potential for remediation of coastal habitats, Mar. Ecol. Prog. Ser., 344, 1–13, doi:10.3354/meps07084, 2007.

Polyakov, I. V., Timokhov, L. A., Alexeev, V. A., Bacon, S., Dmitrenko, I. A., Fortier, L., Frolov, I. E., Gascard, J.-C., Hansen, E., Ivanov, V. V., Laxon, S., Mauritzen, C., Perovich, D., Shimada, K., Simmons, H. L., Sokolov, V. T., Steele, M., and Toole, J.: Arctic Ocean Warming Contributes to Reduced Polar Ice Cap, J. Phys. Oceanogr., 40, 2743–2756, doi:10.1175/2010jpo4339.1, 2010.

Ridgwell, A., Schmidt, D. N., Turley, C., Brownlee, C., Maldonado, M. T., Tortell, P., and Young, J. R.: From laboratory manipulations to Earth system models: scaling calcification impacts of ocean acidification, Biogeosciences, 6, 2611–2623, doi:10.5194/bg-6-2611-2009, 2009.

Riebesell, U., Zondervan, I., Rost, B., Tortell, P. D., Zeebe, R. E., and Morel, F. M. M.: Reduced calcifcation of marine plankton in response to increased atmospheric CO_2, Nature, 407, 365–367, 2000.

Riebesell, U., Schulz, K. G., Bellerby, R. G. J., Botros, M., Fritsche, P., Meyerhofer, M., Neill, C., Nondal, G., Oschlies, A., Wohlers, J., and Zollner, E.: Enhanced biological carbon consumption in a high CO_2 ocean, Nature, 450, 545–548, doi:10.1038/Nature06267, 2007.

Riebesell, U., Czerny, J., von Bröckel, K., Boxhammer, T., Büdenbender, J., Deckelnick, M., Fischer, M., Hoffmann, D., Krug, S. A., Lentz, U., Ludwig, A., Muche, R., and Schulz, K. G.: Technical Note: A mobile sea-going mesocosm system – new opportunities for ocean change research, Biogeosciences, 10, 1835–1847, doi:10.5194/bg-10-1835-2013, 2013.

Rokkan Iversen, K. and Seuthe, L.: Seasonal microbial processes in a high-latitude fjord (Kongsfjorden, Svalbard): I. Heterotrophic bacteria, picoplankton and nanoflagellates, Polar Biol., 34, 731–749, doi:10.1007/s00300-010-0929-2, 2010.

Schippers, P., Lurling, M., and Scheffer, M.: Increase of atmospheric CO_2 promotes phytoplankton productivity, Ecol. Lett., 7, 446–451, doi:10.1111/j.1461-0248.2004.00597.x, 2004.

Schneider, B., Engel, A., and Schlitzer, R.: Effects of depth- and CO_2-dependent C : N ratios of particulate organic matter (POM) on the marine carbon cycle, Global Biogeochem. Cy., 18, GB2015, doi:10.1029/2003gb002184, 2004.

Schulz, K. G., Bellerby, R. G. J., Brussaard, C. P. D., Büdenbender, J., Czerny, J., Engel, A., Fischer, M., Koch-Klavsen, S., Krug, S. A., Lischka, S., Ludwig, A., Meyerhöfer, M., Nondal, G., Silyakova, A., Stuhr, A., and Riebesell, U.: Temporal biomass dynamics of an Arctic plankton bloom in response to increasing levels of atmospheric carbon dioxide, Biogeosciences, 10, 161–180, doi:10.5194/bg-10-161-2013, 2013.

Steinacher, M., Joos, F., Frölicher, T. L., Plattner, G.-K., and Doney, S. C.: Imminent ocean acidification in the Arctic projected with the NCAR global coupled carbon cycle-climate model, Biogeosciences, 6, 515–533, doi:10.5194/bg-6-515-2009, 2009.

Stroeve, J. C., Serreze, M. C., Holland, M. M., Kay, J. E., Malanik, J., and Barrett, A. P.: The Arctic's rapidly shrinking sea ice cover: a research synthesis, Clim. Change, 110, 1005–1027, doi:10.1007/s10584-011-0101-1, 2011.

Svendsen, H., Beszczynska-Møller, A., Hagen, J. O., Lefauconnier, B., Tverberg, V., Gerland, S., Ørbøk, J. B., Bischof, K., Papucci, C., Zajaczkowski, M., Azzolini, R., Bruland, O., Wiencke, C., Winther, J.-G., and Dallmann, W.: The physical environment of Kongsfjorden–Krossfjorden, an Arctic fjord system in Svalbard, Polar Res., 21, 133–166, doi:10.1111/j.1751-8369.2002.tb00072.x, 2002.

Tanaka, T., Alliouane, S., Bellerby, R. G. B., Czerny, J., de Kluijver, A., Riebesell, U., Schulz, K. G., Silyakova, A., and Gattuso, J. P.: Effect of increased pCO_2 on the planktonic metabolic balance during a mesocosm experiment in an Arctic fjord, Biogeosciences, 10, 315–325, doi:10.5194/bg-10-315-2013, 2013.

Thingstad, T. F., Bellerby, R. G. J., Bratbak, G., Borsheim, K. Y., Egge, J. K., Heldal, M., Larsen, A., Neill, C., Nejstgaard, J., Norland, S., Sandaa, R. A., Skjoldal, E. F., Tanaka, T., Thyrhaug, R., and Topper, B.: Counterintuitive carbon-to-nutrient coupling in an Arctic pelagic ecosystem, Nature, 455, 387–390, doi:10.1038/Nature07235, 2008.

Tortell, P. D., Payne, C., Gueguen, C., Strzepek, R. F., Boyd, P. W., and Rost., B.: Inorganic carbon uptake by Southern Ocean phytoplankton, Limnol. Oceanogr., 53, 1266–1278, 2008.

Tremblay, J.-É., Robert, D., Varela, D. E., Lovejoy, C., Darnis, G., Nelson, R. J., and Sastri, A. R.: Current state and trends in Canadian Arctic marine ecosystems: I. Primary production, Climate Change, 115, 161–178, doi:10.1007/s10584-012-0496-3, 2012.

Trenberth, K. E. and Josey, S. A.: Observations: surface and atmospheric climate change, in: Climate Change 2007: The Physical Science Basis: Contribution of Working Group I to the Fourth Assessment Report of the Intergovernmental Panel on Climate Change, edited by: Solomon, S., Qin, D., Manning, M., Chen, Z., Marquis, M., Averyt, K. B., Tignor, M., and Miller, H. L., Cambridge University Press, Cambridge, UK, 235–336, 2007.

Wassmann, P., Duarte, C. M., AgustÍ, S., and Sejr, M. K.: Footprints of climate change in the Arctic marine ecosystem, Glob. Change Biol., 17, 1235–1249, doi:10.1111/j.1365-2486.2010.02311.x, 2011.

Weiss, R. F.: Carbon dioxide in water and sea water: The solubility of a non ideal gas, Mar. Chem., 2, 203–215, 1974.

Welschmeyer, N. A.: Fluorometric analysis of chlorophyll a in the presence of chlorophyll *b* and pheopigments, Limnol. Oceanogr., 39, 1985–1992, 1994.

Wolf-Gladrow, D. A., Zeebe, R. E., Klaas, C., Körtzinger, A., and Dickson, A. G.: Total alkalinity: The explicit conservative expression and its application to biogeochemical processes, Mar. Chem., 106, 287–300, doi:10.1016/j.marchem.2007.01.006, 2007.

Yamamoto-Kawai, M., McLaughlin, F. A., Carmack, E. C., Nishino, S., and Shimada, K.: Aragonite Undersaturation in the Arctic Ocean: Effects of Ocean Acidification and Sea Ice Melt, Science, 326, 1098–1100, doi:10.1126/science.1174190, 2009.

Yamamoto-Kawai, M., McLaughlin, F. A., and Carmack, E. C.: Effects of ocean acidification, warming and melting of sea ice on aragonite saturation of the Canada Basin surface water, Geophys. Res. Lett., 38, L03601, doi:10.1029/2010gl045501, 2011.